Table I. Crystallographic Data for 2a

formula	$C_{25}H_{15}O_4Re$
fw	565.6
cryst syst	orthorhombic
space group	$P2_12_12_1$
a, Å	11.404 (2)
b, Å	12.411 (2)
c, Å	14.499 (2)
V, Å^3	2052.2 (6)
Z	4
density (calcd), g/cm^3	1.830
cryst size, mm	0.3 × 0.4 × 0.4
data collecn instrument	Siemens R3m/V
radiation	Mo Kα (λ = 0.710 73 Å) graphite monochromated
linear abs coeff, cm^{-1}	60.28
temp, °C	−105
scan method	2θ–θ
2θ range, deg	2.0–57.0
F_{000}	1088
p factor used in weighting	0.003 225
no. of unique data	5753
no. of data with $F > 8.0\sigma(F)$	4933
no. of variables	268
$R(F)^a$	4.71
$R_w(F)^b$	7.06
GOF	1.22

$^a R = \sum|F_o - F_c|/\sum|F_o|$. $^b R_w = [|w(F_o - F_c)|^2]^{1/2}/[\sum w|F_o|^2]^{1/2}$.

7. Reaction of 2 with Diethylacetylenedicarboxylate. **2**, 0.15 g (0.26 mmol), and 0.1 mL (0.55 mmol) of diethylacetylenedicarboxylate were refluxed in hexane until the green color disappeared after 2 h. The solvent was pumped off to dryness and the resulting residue recrystallized from hexane at −30 °C yielding **6b** as pale yellow crystals (73% yield).

6b: IR (hexane) ν(CO) 2034 st, 1955 st, 1942 st, 1732 m (C=O); ^{1}H NMR (acetone-d_6) δ 7.29–7.06 mult (15 H), 4.22 q (7 Hz, 4 H), 1.18 t (7 Hz, 6 H); ^{13}C{^{1}H} NMR (acetone-d_6) δ 194.56 (CO), 163.75 (C=O), 133.83, 133.38, 130.74, 130.67, 129.74, 129.45, 129.05 (Ph), 111.97, 111.27, 95.99 (Cp), 62.84 (CH_2), 14.00 (CH_3).

8. Crystallographic Study. Single crystals were grown by cooling a hexane solution of **2** to −30 °C. A suitable crystal was sealed in a thin-walled capillary and mounted on a Siemens R3m/V diffractometer equipped with a low-temperature device. Pertinent crystallographic data are given in Table I. Cell constants and an orientation matrix for data collection were obtained from 25 centered reflections in the range 25.0° < 2θ < 30.0°. Systematic absences indicated the space group to be $P2_12_12_1$. The data were collected at −105 °C by using 2θ–θ scan techniques. Mo Kα radiation was used. The scan rate varied from 2.00 to 15.00°/min in 2θ. The Re atom was located after a Patterson search; all other non-hydrogen atoms were located from difference Fourier syntheses and refined by full-matrix least-squares methods. All non-hydrogen atoms were refined anisotropically. Hydrogen atoms were placed in idealized positions and refined isotropically. The final R values were calculated for $R(F)$ = 4.71 and $R_w(F)$ = 7.06.

Acknowledgment. We thank the Swiss National Foundation for support of this research.

Supplementary Material Available: Tables of crystal data and data collection parameters, atomic coordinates, and thermal parameters and complete lists of bond distances and angles for **2** (8 pages); a structure factor table for **2** (19 pages). Ordering information is given on any current masthead page.

Bonding and Conformational Aspects of Thiolato-Bridged Early–Late Heterobimetallics

Roger Rousseau and Douglas W. Stephan*

Department of Chemistry and Biochemistry, University of Windsor, Windsor, Ontario, Canada N9B 3P4

Received March 1, 1991

Summary: Extended Huckel and Fenske–Hall MO calculations have been used to examine the bonding in a series of thiolato-bridged early–late heterobimetallics. The calculations support the postulate of a weak, dative interaction between the electron-rich late metal and the electron-deficient early metal center. Generally, for Ti species the interaction is weak σ bonding in character, although for Zr there is an indication of an additional π component. When the coordination sphere of the late metal center is trigonal or square planar, these interactions result in a MS_2M' core folding and an *endo–cisoid* conformation of the substituents on the bridging S atoms is adopted. Alternatively, a endo–transoid conformation and a planar MS_2M' core is seen when the late metal center requires a pseudotetrahedral coordination geometry. The implications of these results with respect to the structural and electrochemical properties is considered.

Studies of homogeneous complexes containing both an early, oxophilic and a late electron-rich metal center have been spawned by the observation of strong metal-support interactions (SMSI) in heterogeneous catalyst systems.[1] One postulate offered to explain the phenomenon of SMSI is electronic interaction between the disparate metal centers. Efforts to mimic such interactions have led to the synthesis and study of a series of homogeneous systems containing these diverse metal combinations. As part of our effort in this area, we have previously reported a variety of complexes in which thiolato ligands bridge divergent metal centers. These complexes include species of the form $[Cp_2M(\mu\text{-}SR)_2CuPR_3]^+$ (M = Ti, V) (A),[2,3]

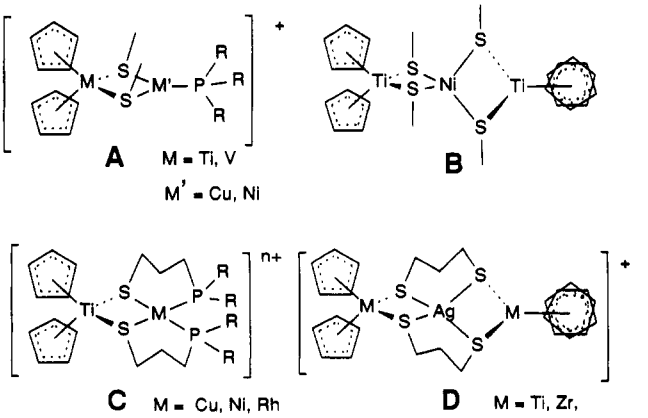

$[Cp_2Ti(\mu\text{-}SR)_2Cu(NCMe)_2]^+$ and $[Cp_2Ti(\mu\text{-}SR)_2]_2Ni$ (B),[3,4]

(1) (a) *Metal-Support Interactions in Catalysis, Sintering, and Redispersion*; Stevenson, S. A., Dumesic, J. A., Baker, R. T. K., Ruckenstein, E., Eds.; Van Nostrand Reinhold Co.: New York, 1987. (b) *Strong Metal-Support Interactions*; Baker, R. T. K., Tauster, S. J., Dumesic, J. A., Eds.; American Chemical Society; Washington, DC, 1986.

(2) Wark, T. A.; Stephan, D. W. *Inorg. Chem.* **1987**, *26*, 363.

0276-7333/91/2310-3399$02.50/0

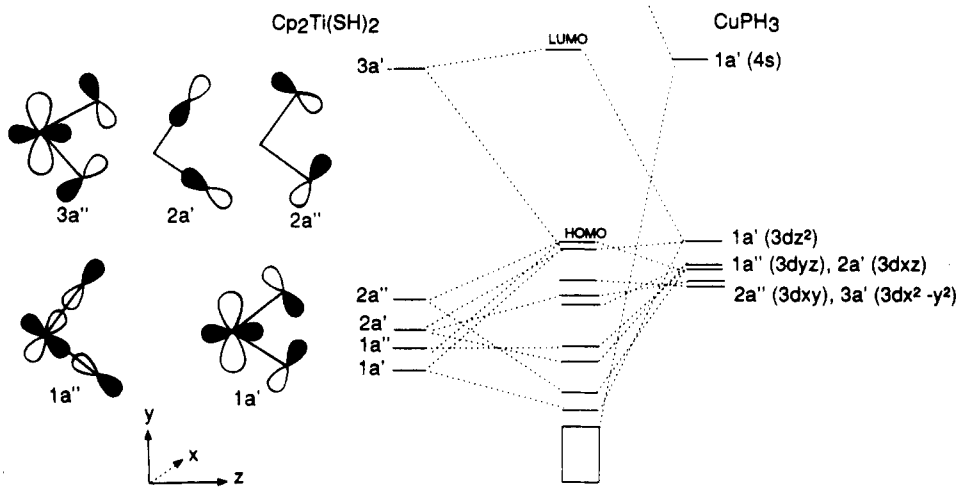

Figure 1. EHMO bonding scheme for 1′. The frontier orbitals for $Cp_2Ti(SH)_2$ and the Cu d orbitals for $[CuPH_3]^+$ are shown.

and $[Cp_2Ti(\mu\text{-}S(CH_2)_nPPh_2)_2M]^{m+}$ (n = 2, 3; M = Cu,[5] Ni,[6] Rh[7]) (C), which have been prepared and structurally characterized. Related early–late Nb–Mo species,[8] as well as, Nb/Ni and Ta/Pt heterotrimetallic complexes are also known.[9] More recently, we have developed related macrocyclic systems of the form $[(Cp_2M(\mu\text{-}S(CH_2)_nS)_2MCp_2)M']^+$ (M = Ti,[10] Zr;[11,12] M′ = Ag, Cu; n = 2,3) (D). The structural and conformational features of these molecules suggest the presence of dative bonding between the early, oxophilic and late, electron-rich transition-metal centers. In this report we describe the results of molecular mechanics and molecular orbital calculations on model compounds derived from the structurally characterized species. The varying conformational preferences observed in thiolato-bridged complexes is addressed and the nature of the interactions between the metals in these species is clarified. Comparisons are made to related studies, and the implications of these results are considered.

Calculations

EHMO and FHMO calculations were performed on model compounds derived from published crystallographic data for $[Cp_2M(\mu\text{-}SEt)_2CuPR'_3]^+$ (M = Ti, R = Ph (**2a**), Cy (**2b**)),[2] $[Cp_2Ti(\mu\text{-}SMe)_2Cu(NCMe)_2]^+$ (**3**),[3] $[Cp_2Ti(\mu\text{-}SR)_2]_2Ni$ (**4**),[4] $[Cp_2Ti(\mu\text{-}S(CH_2)_nPPh_2)_2M]^{m+}$ (M = Cu (**5**),[5] Ni (**6**),[6] Rh (**7a**)[7]), $[(Cp_2Ti(\mu\text{-}SCH_2CH_2CH_2S)_2TiCp_2)Ag]^+$ (**8**),[10] and $[(Cp_2Zr(\mu\text{-}S(CH_2)_nS)_2ZrCp_2Ag]^+$ (n = 2 (**9a**), 3 (**9b**)).[11,12] The model, $Cp_2Ti(SH)_2$ fragment 1′ is used to mimic the $Cp_2Ti(SR)_2$ (1) metalloligand fragments of the ELHB species. The geometry of 1′ was derived from the metalloligand portion of **2a**. C_s symmetry was used in the case of 1′ and **3** but was neglected in all other cases. All R groups on phosphorus and sulfur were replaced by H, employing P–H and S–H distances of 1.42 and 1.30 Å, respectively.[5,6] In the case of the trimetallic complexes the models of the form $[Cp_2M(\mu\text{-}SH)M'(SH_2)_2]^+$ were employed to reduce the size of the calculation. For the EHMO calculations, the implementation of Hoffmann's FORTICON8 resident in the package TRIBBL[13] was employed. Geometry optimizations were performed employing the OPT9 portion of TRIBBL. A detailed description of the Fenske–Hall nonempirical MO method can be found elsewhere.[14] In both cases the calculations were done on a VAX 3520 workstation operating under the VMS operating system. Molecular mechanics calculations were performed by employing the commercially available PC-Model-Pi[15] operating on a IBM AT compatible equipped with 80386 and 80387 processors.

Results and Discussion

Metalloligands. $Cp_2M(SH)_2$ (M = Ti (1′)). This molecular fragment constitutes a model for the metalloligand portion of thiolato-bridged ELHB complexes. A detailed examination of the bonding in titanocenedithiolates has been reported by Calhorda et al.[16] These authors have identified a marked dependence of the total energy on the S–Ti–S angle. As both the Ti–S bond distances and the S–Ti–S angle are increased in the heterobimetallics relative to the those in discrete titanocenedithiolates, these structural changes cause the metalloligand fragment to be of an energy higher than that of the free molecule. Nonetheless, the nature and symmetry of the frontier orbitals of 1′ unaltered (Figure 1).

In considering the interactions of this metalloligand with a late-metal center, three molecular orbitals are most important. The HOMO (2a″) of the metalloligand is primarily composed of the p orbitals on sulfur, which are geometrically disposed so as to provide a σ interaction with a d orbital on a late-metal fragment. Thus it is this orbital that accounts for the ability of titanocenedithiolates to act as metalloligands. The LUMO is similar to the $1a^1$ frontier orbital of Cp_2M described by Hoffmann and Lauher.[17] The structural differences between the metalloligand fragment and free $Cp_2Ti(SH)_2$ cause an increase in the amount of d_{z^2} and p_z character in the LUMO relative to the LUMO of free 1. This results in an increased ability

(3) Wark, T. A.; Stephan, D. W. *Inorg. Chem.* **1990**, *29*, 1731.
(4) Wark, T. A.; Stephan, D. W. *Organometallics* **1989**, *8*, 2836.
(5) White, G. S.; Stephan, D. W. *Inorg. Chem.* **1985**, *24*, 1499.
(6) White, G. S.; Stephan, D. W. *Organometallics* **1988**, *7*, 903.
(7) White, G. S.; Stephan, D. W. *Organometallics* **1987**, *6*, 2169.
(8) Darensbourg, M. Y., Silva, R.; Reibenspies, J.; Prout, C. K. *Organometallics* **1989**, *8*, 1315.
(9) (a) Douglas, W. E.; Green, M. L. H.; Prout, C. K.; Rees, G. V. *J. Chem. Soc., Chem. Commun.* **1971**, 896. (b) Prout, C. K.; Critchley, S. R.; Rees, G. V. *Acta Crystallogr., Sect. B* **1974**, *30*, 2305. (c) Daran, J. C.; Meunier, B.; Prout, K. *Acta Crystallogr., Sect. B* **1979**, *35*, 1709.
(10) Nadasdi, T. T.; Stephan, D. W. *Organometallics*, submitted for publication.
(11) Stephan, D. W. *J. Chem. Soc., Chem. Commun.* **1991**, 121.
(12) Stephan, D. W. *Organometallics* **1991**, *10*, 2037.
(13) Pensak, D. A.; Wendoloski, J. J. Quantum Chemistry, Program Exchange, Program No. 529.
(14) Hall, M. B.; Fenske, R. F. *Inorg. Chem.* **1972**, *11*, 768.
(15) Available from Serrena Software, Bloomington, IN.
(16) Calhorda, M. J.; Carrondo, M. A. F. C. T.; Dias, A. R.; Frazao, C. F.; Hursthouse, M. B.; Simoes, J. A. M.; Teixeira, C. *Inorg. Chem.* **1988**, *27*, 2513.
(17) Hoffmann, R.; Lauher, J. *J. Am. Chem. Soc.* **1976**, *98*, 1729.

Table I. Thiolato-Bridged ELHB Complexes, Models, and Net Overlap Population from FHMO Calculations

compd	M–M′	ref	model	M–M′ NOP
$[Cp_2Ti(\mu\text{-}SEt)_2CuPPh_3]^+$	2.803 (3)	2	$[Cp_2Ti(\mu\text{-}SH)_2CuPH_3]^+$	0.044
$[Cp_2Ti(\mu\text{-}SEt)_2CuPCy_3]^+$	2.840 (2)	2		
$[Cp_2Ti(\mu\text{-}SEt)_2Cu(NCMe)_2]^+$	2.847 (2)	3	$[Cp_2Ti(\mu\text{-}SH)_2Cu(NH_3)_2]^+$	0.035
$Cp_2Ti(\mu\text{-}SMe)_2Mo(CO)_4$	3.321 (2)	24	$[Cp_2Ti(\mu\text{-}SH)_2Cu(PH_3)_2]^+$	0.010
$[Cp_2Nb(\mu\text{-}SPh)_2Mo(CO)_4]^+$	3.116 92)	8	$Cp_2Ti(\mu\text{-}SH)_2Mo(CO)_4$	0.025
$[Cp_2Ti(\mu\text{-}SCH_2CH_2PPh_2)_2Cu]^+$	3.024 (1)	5	$Cp_2Nb(\mu\text{-}SH)_2Mo(CO)_4$	0.110
$[Cp_2Ti(\mu\text{-}SCH_2CH_2CH_2PPh_2)_2Ni]$	2.825 (3)	6	$Cp_2Ti(\mu\text{-}SH)_2Ni(PH_3)_2$	0.060
$[Cp_2Ti(\mu\text{-}SCH_2CH_2CH_2PPh_2)_2Rh]^+$	3.127 (2)	7	$[Cp_2Ti(\mu\text{-}SH)_2Rh(PH_3)_2]^+$	0.032
$(Cp_2Ti(\mu\text{-}SMe)_2)_2Ni$	2.786 (1)	4	$[Cp_2Ti(\mu\text{-}SH)_2Ni(SH_2)_2]^+$	0.075
$[(Cp_2Ti(\mu\text{-}SCH_2CH_2CH_2S)_2TiCp_2)Ag]^+$	3.207 (7)	10	$[Cp_2Ti(\mu\text{-}SH)_2Ag(SH_2)_2]^+$	0.025
	3.246 (7)			
	3.264 (6)			
	3.279 (6)			
$[(Cp_2Zr(\mu\text{-}SCH_2CH_2S)_2ZrCp_2)Ag]^+$	3.047 (2)	12	$[Cp_2Zr(\mu\text{-}SH)_2Ag(SH_2)_2]^+$	0.080
	3.058 (2)			
$[(Cp_2Zr(\mu\text{-}SCH_2CH_2CH_2S)_2ZrCp_2)Ag]^+$	3.333 (3)	11, 12	$[Cp_2Zr(\mu\text{-}SH)_2Ag(SH_2)_2]^+$	0.027
	3.280 (3)			
$[(Cp_2Nb(\mu\text{-}SMe)_2)_2Ni]^{2+}$	2.765 (5)	9a,b		
	2.776 (5)			
$[(Cp_2Ta(\mu\text{-}SMe)_2)_2Pt]^{2+}$	2.788 (1)	9c		
	2.809 (7)			

of the LUMO to act as a σ acceptor from an electron-rich late metal. The orbital, which is primarily the d_{xz} orbital of titanium, is of correct symmetry to allow for a π-bonding interaction with a late-metal center; however, it should be noted that this orbital is significantly higher in energy than late-metal d orbitals and thus is not likely to afford a significant interaction.

Bimetallic Systems. $[Cp_2Ti(\mu\text{-}SH)_2CuPH_3]^+$ (2′). The d orbitals of $[CuPH_3]^+$ and the EHMO diagram for the interaction of the $[CuPH_3]^+$ fragment with the metalloligand 1′ are shown in Figure 1. The primary link between the two fragments involves the interaction of the 1a′ and 2a″ of 1′ with the 3a′ and 1a″ acceptor orbitals of $[CuPH_3]^+$, respectively. This, of course provides the Cu–S bonds. It is however, the degree and nature of the direct Ti–Cu interaction that is of most interest. The Ti–Cu distance is 2.803 (3) Å. This distance is the shortest Ti–M separation seen in thiolato-bridged ELHB complexes. The MO calculations show a σ interaction involving d_{z^2} on Cu and the spd_{z^2} portion of the $1a_1$ and $2a_1$ orbitals on Ti, resulting in the second highest occupied molecular orbital. The σ-bonding orbital for 1′ is shown in Figure 2b. It is clear from this plot that Cu–Ti bonding is significantly weaker than the Cu–P bonding; and in fact, EHMO calculations predict a negative M–M′ overlap population for the related species $Cp_2Th(\mu\text{-}PH_2)_2Ni(CO)_2$.[18] This, however, may arise as a result of counterintuitive orbital mixing.[19] Thus FHMO calculations were undertaken to better assess the degree of metal–metal interactions. The results of FHMO calculations are consistent with the EHMO results except that the M–M′ σ interaction appears as the HOMO in the FHMO scheme. The degree of M–M′ bonding cannot be quantitatively assessed with accuracy by FHMO calculations; however the net overlap population (NOP) serves as a qualitative and comparative guide. In the case of 2′, the NOP is positive (Table I) between Ti and Cu, thus indicating an overall bonding character between the metals. The Ti–Cu σ orbital lies 28% on Ti and 30% on Cu, while the related σ antibonding LUMO lies 55% on Ti and 10% on Cu. No π interaction occurs between the Ti and the d_{xz} orbital on Cu. As a point of reference, FHMO calculations of the NOP between the metal centers in $Cp_2(OH)ZrRuCp(CO)_2$[20] were found to be

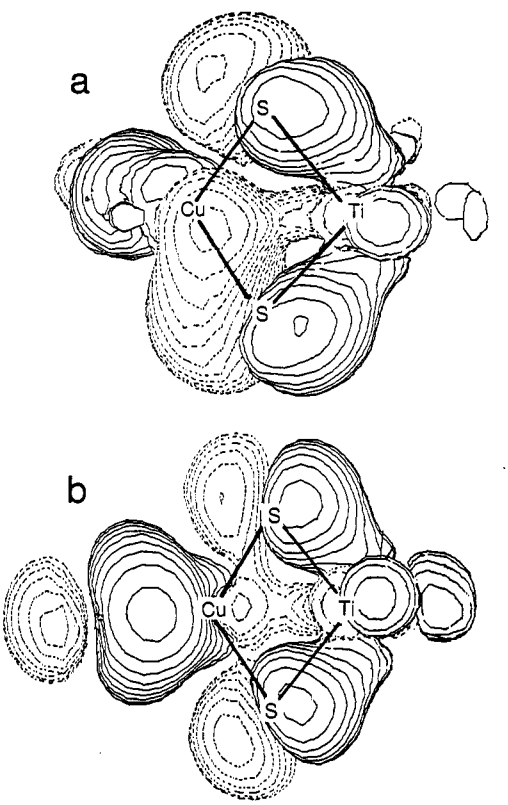

Figure 2. (a) Three-dimensional contour depiction of the σ-bonding Ti–Cu orbital in 3′ and (b) in 1′. Solid and dashed contour lines are used to represents the differing phases of the lobes. In each case, the view of the three-dimensional orbital plot is perpendicular to the TiS_2Cu plane. The plotted contours are derived from EHMO calculations.

0.410. This suggests that while the Ti–Cu interaction indicated for 2′ is certainly bonding, it is weak.

An extended Huckel total energy minimization calculation was preformed in which only the dihedral angle between the S–Ti–S and S–Cu–S planes was allowed to vary. The starting point was a planar TiS_2Cu core. Nonetheless, a puckered or "butterflied" core with a angle of 15° between the MS_2 planes yields the energetically preferred geometry.[2] This agrees well with the results of

(18) Ortiz, J. V. *J. Am. Chem. Soc.* **1986**, *108*, 550.
(19) Ammeter, J. H.; Burgi, H. B.; Thibeault, J. C.; Hoffman, R. *J. Am. Chem. Soc.* **1978**, *100*, 3686.
(20) Casey, C. P.; Jordan, R. F.; Rheingold, A. L. *J. Am. Chem. Soc.* **1983**, *105*, 665.

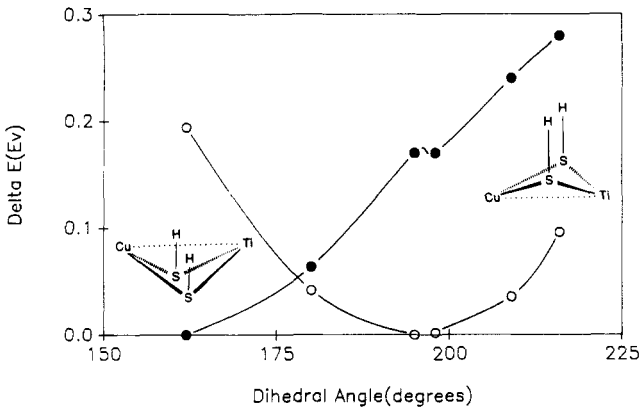

Figure 3. Plot of total energy of 1′ as a function of core folding at sulfur (○). The energy of the σ-bonding Ti–Cu orbital is also shown (●).

the crystallographic study. This puckered or butterflied TiS_2Cu core lies 0.3 eV lower in total energy than the planar form and at the same time increases the M–M′ interaction. Although further folding of the core results in an decrease in the energy of the Cu–Ti σ orbital, the total energy in increased. This undoubtedly reflects the conflicting energetics of the stabilizing Cu–Ti interaction with the destabilizing ring strain within the CuS_2Ti core (Figure 3). This is in marked contrast to results of several related studies. Hay[21] performed calculations for the model $Cl_2Th(\mu\text{-}PH_2)_2PtPH_3$ to investigate the actinide–metal bonding in $Cp_2Th(\mu\text{-}PPh_2)_2PtPPh_3$, while Baker et al.[22] have described EHMO calculations for models of the form $Cp_2Zr(\mu\text{-}PH_2)_2M'L_n$. In both systems, puckering of the MP_2M' core results in no electronic stabilization, and in fact, the planar geometries were found to be more stable in those cases.

$[Cp_2Ti(\mu\text{-}SH)_2Cu(PH_3)_2]^+$ (5′) and $[Cp_2Ti(\mu\text{-}SH)_2Ni(PH_3)_2]$ (6′). The late-metal fragments in these d^0–d^{10} systems adopt a pseudotetrahedral geometry. As expected, the MO schemes from these two models are very similar in form and, in addition, the FHMO and EHMO calculations agree remarkably well for these ELHB species. M–M′ interactions of a σ nature occur between the $1a_1/2a_1$ and the $p_zd_{z^2}$ orbitals on both Ti and Cu (Ni), respectively. In the case of 5′, this σ orbital appears as the second highest occupied molecular orbital and lies 17% on Ti and 72% on Ni. The LUMO, which is the σ* orbital, is 40% located on Ti and 38% on Ni. The calculations indicate no π interaction between the two metal centers. Qualitatively, the net overlap populations between the two metal centers (6′, 0.060; 5′, 0.010) are consistent with the significantly longer Ti–Cu separation in **5** (3.024 (1) Å)[5] compared to the Ti–Ni distance (2.825 (3) Å) in **6**.[6] This can be attributed, in part, to the charge on Cu, which presumably diminishes electron donation to empty Ti acceptor orbitals.

Optimizations of the dihedral angle between the two S–M–S planes, based on a minimization of the total energy, showed only a minimal distortion (2°) from planarity. Distortion of the TiS_2M' cores of these models are inhibited by the repulsion between the cyclopentadienyl ligands and the substituents on P and S. Shorter Ti–M′ distances afford significantly increased net overlap populations between the two metals; however, as both of the original models were derived from crystallographically characterized species containing chelating, phosphine–thiolate ligands, it appears that geometric constraints of the chelates act to restrict the degree of dative interaction between the metal centers. Further support for this reasoning is given by both the structural data for $[Cp_2Ti(\mu\text{-}SEt)_2Cu(NCMe)_2]^+$ (**3**), which shows that in the absence of the chelating ligand the approach of the pseudotetrahedral Cu and the Ti atoms is 2.847 (2) Å.[3] FHMO calculations for the corresponding model, $[Cp_2Ti(\mu\text{-}SH)_2Cu(NCMe)_2]^+$ (3′) show a net overlap population between Ti and Cu of 0.035. The σ-bonding orbital for 3′ is shown in Figure 2a.

$[Cp_2Ti(\mu\text{-}SH)_2Rh(PH_3)_2]^+$ (7′). The frontier orbitals of the $[Rh(PH_3)_2]^+$ fragment are similar to those of the $[M(PH_3)_2]$ fragments described above. However, the interaction of this fragment with the metalloligand fragment, $Cp_2Ti(SH)_2$, occurs at 90° relative to the analogous interactions in 4′ and 5′. EHMO calculations place the Ti–Rh σ orbital as the second highest occupied molecular orbital and the HOMO when C_s symmetry is imposed. An optimization of the dihedral angle between the MS_2 planes predicts a fold of 8°, which compares well with the crystal data. These results imply that perturbations of the core geometry and distortions from C_s symmetry stabilize the Ti–Rh interaction and reduce the total energy as well. Again this is contrary to results reported for phosphido-bridged systems. FHMO calculations place the σ orbital lower in energy, below the three rhodium d, centered orbitals, lying 82% on Rh and 13% on Ti. Despite this difference, EHMO and FHMO calculations are consistent in identifying the LUMO as the antibonding σ* orbital and in predicting no π interaction between the metal centers.

Redox Properties. The LUMO for 2′, 5′, and 7′ is largely Ti based and M–M′ antibonding in character. Population of this orbital by electrochemical or chemical reduction is possible for **2** and **7**, affording the reduced species $[Cp_2Ti(\mu\text{-}SCH_2CH_2PPh_2)_2Cu]$ (**3b**)[5] and $[Cp_2Ti(\mu\text{-}SCH_2CH_2CH_2PPh_2)_2Rh]$ (**7b**),[7] respectively. Population of the LUMO by chemical reduction is only tolerated by the complexes containing the S–P chelating ligands, suggesting that the M–M′ interaction is a stabilizing factor in the oxidized forms. However, the compounds $[Cp_2V(\mu\text{-}SEt)_2CuPR_3]^+$ (**2c**),[3] are isoelectronic with the reduction product of **2** and are isolable. Although not well suited for open-shell molecules, calculations for the reduced species **7b** indicate a small but discernible net overlap population between Ti and Rh. This is consistent with the postulate that transannular interactions account for the observation of hyperfine coupling between Ti and Rh in **7a** as well as the Cu hyperfine coupling observed for **2c**.[5,7] Reversible oxidations observed for **6** were attributed to the Ni(0)/Ni(I) and Ni(I)/Ni(II) redox couples.[6] This assignment is supported by the present calculations which identify the HOMO is largely Ni d orbital in character.

Trimetallic Systems. The analysis of the trimetallic systems 4′ and 8′–10′ is qualitatively similar to that described above. In the case of **4**, the Ti–Ni distances are similar to that seen in **6**,[4,6] and a similar NOP is calculated despite the fact that two Ti atoms are present to act as acceptors for electron density at Ni. This is in contrast to the related phosphido-bridged species $(Cp_2Zr(\mu\text{-}PPh)_2)_2Ni$ where the Zr–Ni distance is much longer than that seen in related bimetallics.[22] It appears that the steric demands of four phosphido groups about the central Ni atom inhibit the approach of the metal centers and thus diminish M–M′ interactions. Such is not the case for the thiolato-bridged species. Nonetheless, the M–M′ distances and thus degree of interaction are altered when a intervening chelate chain restricts the M–M′ approach, as in

(21) Hay, P. J.; Ryan, R. R.; Salazar, K. V.; Wrobleski, D. A.; Sattelberger, A. P. *J. Am. Chem. Soc.* **1986**, *108*, 313.
(22) Baker, R. T.; Fultz, W. C.; Marder, T. B.; Williams, I. D. *Organometallics* **1990**, *9*, 2357.

$[(Cp_2Zr(\mu\text{-}SCH_2CH_2CH_2S)_2ZrCp_2)Ag]^+$.[11,12] In addition, FHMO calculations for Zr or Nb thiolato-bridged models show that as the second row metal d orbitals are lower in relative energy compared to Ti, larger overlap populations despite longer M–M′ distances, are observed. In addition, both σ and π components comprise the interactions between Zr or Nb and the late metals. Similar results were observed for the models $Cp_2Zr(\mu\text{-}PH_2)_2ML_n$.[22]

Conformational Considerations. Three conformers are possible for the free metalloligands; *cisoid–endo*, *transoid–endo*, and *exo*. Structural data reveal that free titanocenedithiolates $Cp_2Ti(SR)_2$ (R = Me, Et) adopt the

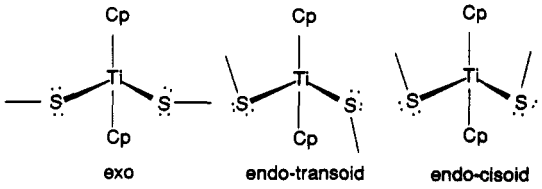

endo–transoid conformation. This preference has been rationalized on the basis of both electronic and steric arguments.[2] In contrast, Darensbourg et al.[23] have shown that the *exo* conformation is preferred by d^1 and d^2 complexes of the form $Cp_2M(SR)_2$. On binding to the late-metal center, only *endo* conformations of the titanocenedithiolate moieties are geometrically and sterically permitted. The structural data for **2** show that the ethyl substituents adopt a *cisoid–endo* conformation. Restricted MMX calculations were performed for **2** in which the metal atom geometries were held constant and only the organic substituents on S and P were allowed to vary. The results confirm a qualitative energetic preference for the *cisoid–endo* over the *transoid–endo* conformer. In contrast, related qualitative, restricted MMX calculations for **2** in which the TiS_2Cu core was constrained to be planar, shows an energetic preference for the *transoid–endo* conformer. Thus, it seems that the fold in the TiS_2Cu core, which accommodates Ti–Cu bonding, enhances the preference for a *cisoid* conformation.

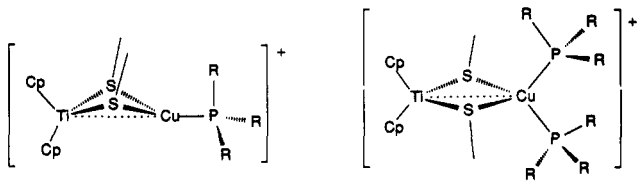

A similar result is also seen for **7**. In contrast to **2** and **7**, the pseudotetrahedral coordination spheres of Cu(I) and Ni(0) in **5** and **6**, respectively, requires a *transoid–endo* sulfur substituent conformation and thus planar MS_2M' cores are observed. This is also true for the trimetallic species with central d^{10} metal centers.[4,9]

Summary. The EHMO and FHMO calculations establish that a weak, dative, metal–metal interaction exists in these thiolato-bridged heterobimetallics. Generally, for Ti species the interaction is weak and σ bonding in character, although for Zr there is an indication of an additional π component. When the coordination sphere of the late-metal center is trigonal or square planar, these interactions result in a MS_2M' core folding and an *cisoid–endo* conformation of the substituents on the bridging S atoms is adopted. Alternatively, a *transoid–endo* conformation and a planar MS_2M'core are seen when the late-metal center requires a pseudotetrahedral coordination geometry. In any case, the approach of the metal centers is affected by steric factors. The ramifications of such metal–metal interactions on the chemistry of ELHB species is the subject of on-going study.

Acknowledgment. Financial support from NSERC of Canada is gratefully acknowledged. The University of Windsor is thanked for the award of a Research Professorship (D.W.S.).

(23) Darensbourg, M. Y.; Bischoff, C. J.; Houliston, S. A.; Pala, M.; Reibenspies, J. *J. Am. Chem. Soc.* **1990**, *112*, 6905.
(24) (a) Cameron, T. S.; Prout, K. C.; Rees, G. V.; Green, M. L. H.; Joshi, K. K.; Davies, G. R.; Kilbourn, B. T.; Braterman, P. S.; Wilson, V. A. *J. Chem. Soc., Chem. Commun.* **1971**, 14. (b) Davies, G. R.; Kilbourn, B. T. *J. Chem. Soc. D* **1971**, 87.

(Trialkylsiloxy)dialkylaluminum Dimers

Rolf Mulhaupt,† Joseph Calabrese, and Steven D. Ittel*
Central Research & Development,‡ E. I. du Pont de Nemours & Company, Wilmington, Delaware 19880-0328
Received May 14, 1991

Summary: Trimethylaluminum reacts with cyclic siloxane oligomers or poly(siloxanes) to generate the primary member of a family of dimeric dialkylaluminum trialkylsiloxanes, (trimethylsiloxy)dimethylaluminum, $[Me_2Al(OSiMe_3)]_2$. The X-ray crystal structure of this primary siloxalane has been redetermined with use of modern crystallographic techniques. It crystallizes in the space group $C2/m$ (No. 12) with unit cell dimensions a = 11.350 (5) Å, b = 13.101 (2) Å, c = 6.918 (4) Å, and β = 111.60 (2)°.

There has been considerable work demonstrating that alkylaluminum reagents modified by reaction with a wide variety of siloxanes are useful in the preparation of Ziegler–Natta catalysts[1] and catalysts for olefin metathesis.[2] The polymerization catalysts display high activity for ethylene polymerization and high activity and stereospecificity in the polymerization of propene. In one remarkable issue of *Chemical Abstracts Selects*[3] there were

† Current address: Institut für Makromolekulare Chemie, Stefan Meier Str. 31, D-7800 Freiburg i. Br., Germany.

‡ Contribution No. 5653.

(1) For good examples of commercial use applications, see: (a) Schmidt, M.; Schmidbaur, H. (Wasag-Chemie AG). U.S. Patent 3,373,178, 1968. (b) Gloriod, P.; Levresse, B.; Machon, J.-P. (Ethylene Plastique). U.S. Patent 3,969,332, 1976. (c) Piekarski, G.; Hundmeyer, A.; Kippe, D.; Maier, S. (Wacker Chemie GmbH). U.S. Patent 3,755,274, 1973. (d) Miyanishi, H.; Shimada, T.; Hayashi, S.; Matsuura, M.; Fujita, T.; Matsui, R.; Kageyama, Y. (Mitsubishi). U.K. Patent Appl. GB 2,057,468, 1980. (e) Machon, J. P.; Hermant, R.; Houzeaux, J. P. *J. Polym. Sci., Polym. Symp.* **1975**, *52*, 107. (f) Hamilton, M. A.; Harbourne, D. A.; Russell, C. G.; Zboril, V. G.; Mulhaupt, R. (Du Pont Canada). EP131,420, 1988.

0276-7333/91/2310-3403$02.50/0